Optics Letters

Pilot-tone-based self-homodyne detection using optical nonlinear wave mixing

Yinwen Cao,[1,*] Morteza Ziyadi,[1] Ahmed Almaiman,[1] Amirhossein Mohajerin-Ariaei,[1] Peicheng Liao,[1] Changjing Bao,[1] Fatemeh Alishahi,[1] Ahmad Fallahpour,[1] Bishara Shamee,[1] Asher J. Willner,[1] Youichi Akasaka,[2] Tadashi Ikeuchi,[2] Steven Wilkinson,[3] Carsten Langrock,[4] Martin M. Fejer,[4] Joseph Touch,[5] Moshe Tur,[6] and Alan E. Willner[1]

[1]Department of Electrical Engineering, University of Southern California, Los Angeles, California 90089, USA
[2]Fujitsu Laboratories of America, 2801 Telecom Parkway, Richardson, Texas 75082, USA
[3]Raytheon Company, El Segundo, California 92195, USA
[4]Edward L. Ginzton Laboratory, 348 Via Pueblo Mall, Stanford University, Stanford, California 94305, USA
[5]Information Sciences Institute, University of Southern California, Marina del Rey, California 90292, USA
[6]School of Electrical Engineering, Tel Aviv University, Ramat Aviv 69978, Israel
*Corresponding author: yinwenca@usc.edu

Received 13 March 2017; accepted 4 April 2017; posted 11 April 2017 (Doc. ID 287889); published 28 April 2017

An all-optical pilot-tone-based self-homodyne detection scheme using nonlinear wave mixing is experimentally demonstrated. Two scenarios are investigated using (1) multiple wavelength-division-multiplexed channels with sufficient power of the pilot tones and (2) a single channel with a low-power pilot tone. The eye diagram and bit error rate of the system are studied by tuning various parameters such as pump power, relative phase, and pilot-to-signal ratio.

OCIS codes: (060.2920) Homodyning; (060.2360) Fiber optics links and subsystems; (060.4370) Nonlinear optics, fibers.

https://doi.org/10.1364/OL.42.001840

Optical coherent detection is of importance in optical communication systems, especially for the recovery of sensitive phase-encoded data signals [1–3]. A coherent detection system notably requires phase and frequency locking between the incoming signal and the local oscillator (LO). Approaches to achieving a stable locking include the use of an optical phase-locked loop [4–6] or digital carrier recovery [7–10].

Self-homodyne detection (SHD) is another approach that can potentially simplify receiver signal processing [11] and relax the requirement for narrow linewidth lasers [12]. One common approach to realizing SHD relies on transmitting a pilot tone, along with the data channel on another frequency or an orthogonal polarization. At the receiver, the pilot tone is extracted and processed in a different path that allows it to later beat with the data channel as an LO laser [11–14]. This approach requires a sufficient pilot-to-signal ratio (PSR) to ensure system performance [15,16], and it is typically accomplished by (1) transmitting a pilot tone with sufficient power, which reduces the effective data signal power that can be accommodated for transmission; or (2) amplifying/regenerating a low-power co-transmitted pilot tone in a separate path at the receiver, which might require a phase-locked loop [13].

Recently, there has been another SHD method proposed using two stages of optical nonlinear wave mixing without sending a pilot tone [17]. By generating the delayed version of the incoming signal conjugate which is later mixed with the original signal, this approach can automatically lock a "local" pump to the signal without requiring a feedback loop controller. However, this approach (1) alters the original data encoding from quadrature-phase-shift-keying (QPSK) to differential QPSK by using an optical differentiator, and (2) might be difficult to extend to a multi-channel wavelength-division-multiplexed (WDM) system.

In this Letter, we demonstrate SHD that combines the use of the co-transmitted pilot tone and optical nonlinear wave mixing at the receiver. Our method is as follows: (1) at the transmitter, a pilot tone is placed at an adjacent frequency to a data channel; and (2) at the receiver, phase-locked optical frequency comb lines are employed to convert the pilot tone to the center of the data channel spectrum [18,19]. This approach uses only a single nonlinear mixing stage to achieve automatic phase locking for SHD without path separation or altering the data encoding. We demonstrate it with multiple WDM channels, each with its own pilot tone. In an experiment, two 20 Gbaud QPSK channels are recovered using a single periodically poled lithium niobate (PPLN) waveguide. To address the power issue of the pilot tone, narrow-band Brillouin amplification (BA) is added at the receiver for inline selective amplification of the pilot tone. This achieves SHD for the channel with an ultralow power pilot tone. We experimentally demonstrate this scheme in a single channel of 10/20 Gbaud BPSK and 10 Gbaud QPSK signals. System performance can be maintained with a PSR as low as −30 dB.

The concept of the proposed SHD system is shown in Fig. 1. At the transmitter, two data channels (S_1 and S_2) are sent with

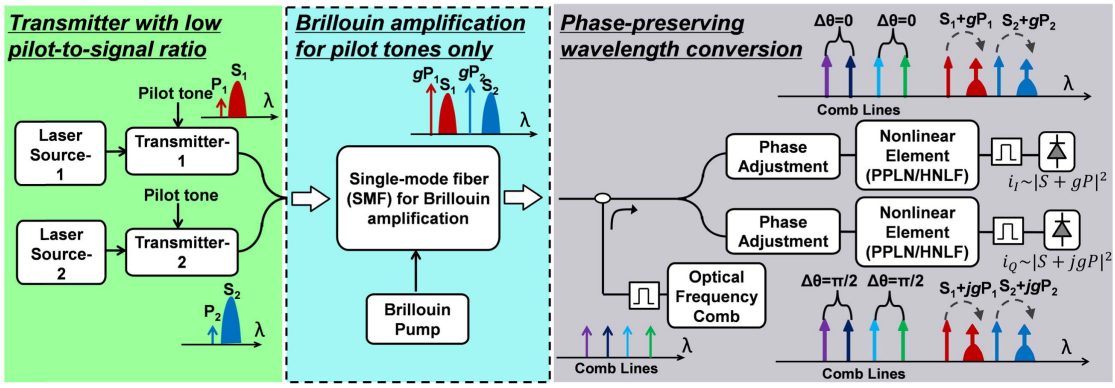

Fig. 1. Conceptual diagram of the proposed SHD system. The scheme is composed of (1) BA to selectively amplify the pilot tones if the PSR is low, and (2) phase-preserving wavelength conversion using optical frequency comb lines. The following two experiments demonstrate SHD for different scenarios: (1) WDM channels with sufficient PSR (without BA) and (2) a single channel with low PSR (with BA). PPLN, periodically poled lithium niobate; HNLF, highly nonlinear fiber.

different pilot tones (P_1 and P_2). At the receiver, if the power of P_1 and P_2 is low (low PSR), a stage of BA is employed to selectively amplify the pilot tone by a gain coefficient of g without needing path separation [20,21]. In the next stage, the data channels (S_1, S_2) and the amplified pilot tones (gP_1, gP_2) are coupled with four phase-locked optical frequency comb lines to achieve phase-preserving wavelength conversion in a genetic nonlinear element, which could be a PPLN or a highly nonlinear fiber (HNLF) [22]. By choosing an appropriate frequency difference (the frequency difference between S_i and P_i, $I = 1, 2$) and relative phase ($\Delta\theta$) between the comb lines, the pilot tones are converted to the center of the data channel. Both I and Q components can be recovered using direct detection.

In the first experiment, the power of the pilot tone is sufficiently high so that the BA can be bypassed. In Fig. 2, a mode-locked laser (MLL) with a 10 GHz repetition rate is injected into a delay line interferometer (DLI) followed by a 450 m HNLF to generate optical frequency comb lines with a broad spectrum, as shown in Fig. 2(b1). A clock synchronizer is employed to maintain the repetition rate with a 10 GHz clock reference. The transmitter and receiver share the comb lines, which are decorrelated by a 30 km single-mode fiber (SMF). In a spatial light modulator (SLM) filter at the transmitter, two comb lines are selected to be sent to an IQ modulator to

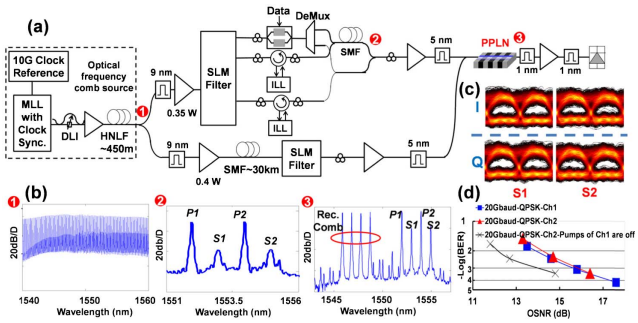

Fig. 2. (a) Experimental setup of SHD for WDM channels with high-power pilot tones without the middle part (BA) of Fig. 1; (b) corresponding spectra at each node; (c) eye diagrams of the two detected 20 Gbaud QPSK channels; (d) BER measurements. MLL, mode-locked laser; DLI, delay line interferometer; ILL, injection-locked laser; SLM, spatial light modulator.

generate 20 Gbaud QPSK signals. On the other port of the SLM filter, two other comb lines are selected as the corresponding pilot tones of the modulated signals. By sending these tones into injection-locked lasers (ILLs), they are amplified at the transmitter. The reason to use ILL is to make the scenario that the pilot tones have sufficient power at the transmitter side, whereas the purpose of this experiment is to focus on the feasibility demonstration of SHD for a multi-channel system. For channel decorrelation, each of the signals with its own pilot tone is sent through different fiber paths and is later combined with a spectrum shown in Fig. 2(b2).

At the receiver, the signals with pilot tones are amplified and sent into a PPLN with a quasi-phase matching wavelength of ~1550.5 nm, along with the receiver's frequency comb lines. Inside the PPLN waveguide, the pilot tones are converted to the center of each of the data channels, as shown in Fig. 2(b3). The desired signal is then filtered and sent to a photodetector (PD) for detection. Due to the path separation between the pilot tone and signal at the transmitter side, an offline digital signal stabilization is employed to compensate for the resultant phase variation based on a decision directed approach [23]. Because our available experimental setup has access to only a single PPLN (in contrast to the concept shown in Fig. 1), the two output paths (I and Q) of Fig. 1 have to be measured separately, each following proper adjustment of $\Delta\theta$ between the comb lines using SLM filter-2, as shown in Fig. 2(a). Figure 2(c) shows the eye diagrams for the two 20 Gbaud QPSK channels. The bit error rate (BER) measurement is shown in Fig. 2(d). Compared to simultaneous multi-channel detection, separate channel detection could achieve a 1.8 dB OSNR improvement at a BER of $1e^{-3}$. The extra penalty might arise from the crosstalk in the PPLN, which is expected to increase if this approach is extended to a larger number of channels. Approaches for effective suppression of the crosstalk require further research in the future.

In the presence of a low-power co-transmitted pilot tone, the BA stage is included to boost power before the nonlinear wave mixing. The experimental setup of a single-channel SHD with a low PSR is shown in Fig. 3(a). At the transmitter, the data are generated using a high-speed arbitrary waveform generator (AWG), and the I component is added with a low-power sinusoidal pilot tone generated by a 40 GHz clock synthesizer. The

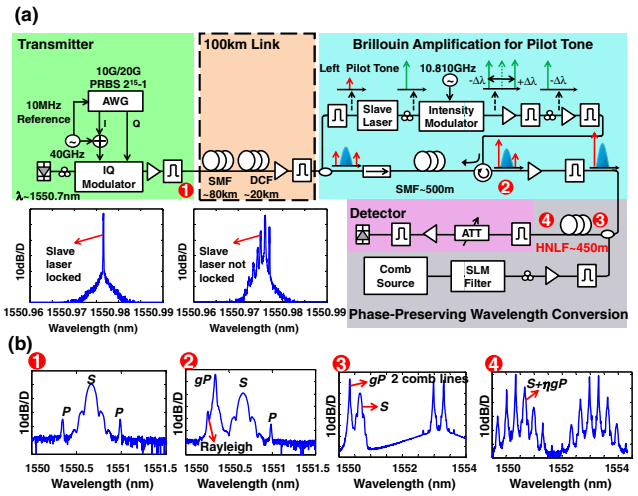

Fig. 3. (a) Experimental setup of SHD for a single channel with a −30 dB PSR and the spectra when the slave laser for BA is frequency locked or unlocked to the incoming pilot tone; (b) corresponding spectra measured at each node.

clock in the AWG is frequency locked with the pilot tone clock by a 10 MHz reference. Then the data signal modulates a laser at the wavelength of 1550.7 nm in an IQ modulator. The spectrum of the signal with a pilot tone is shown in Fig. 3(b1), where the launch power is 3 dBm, and the PSR is −30 dB. The signal with the pilot tone is sent to either (1) the proposed SHD structure directly for B2B evaluation, or (2) a 100 km link compromising an 80 km SMF and a 20 km dispersion compensated fiber with a total loss of 30.7 dB.

At the receiver, the incoming signal with a pilot tone is sent to two paths. In the upper path, the left pilot tone is selected by a narrow-band optical filter and sent to a slave laser that is frequency locked to the input pilot tone. Compared to [24,25], which require a phase locking of ILL, the slave laser is used as a BA pump so that phase locking is not required. The temperature and current of the slave laser need to be tuned for frequency locking. The output is then modulated by a 10.810 GHz sinusoidal tone in an intensity modulator biased at the null point. The generated lower sideband (higher frequency) continuous waveform is selected and amplified to act as the BA pump, as shown in Fig. 3(a). Afterward, the BA pump propagates in the opposite direction to the incoming signal in a 500 m SMF, in which only the pilot tone is amplified by ∼40 dB with the narrow-band Brillouin interaction, as shown in Fig. 3(b2). The signal with a pilot tone is then amplified in an EDFA and sent into a narrow-band optical filter, in which the Rayleigh back-scattering component is suppressed. In the next stage, the same comb sources in Fig. 2(b1) are sent to a SLM filter,

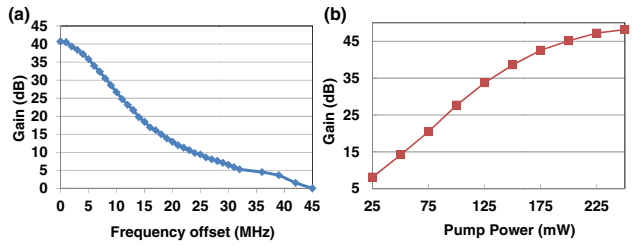

Fig. 4. (a) Bandwidth of Brillion amplification; (b) gain variation of BA for the pilot tone by changing the pump power.

and two comb lines with a 40 GHz frequency difference are selected with appropriate phase adjustment. Then the two comb lines are amplified before sending them to a 450 m HNLF. The complete spectra before and after the HNLF are shown in Figs. 3(b1) and 3(b4), in which the amplified pilot tone is converted to the middle of the data spectrum. In the experiment, the frequency spacing between the signal and a pilot tone is manually tuned to align with the frequency spacing between the two comb lines. For the practical implementation in which the transmitter and receiver are at different locations, a simple digital frequency offset estimation and compensation [26] would be required. Finally, the data channel is filtered and sent to a PD for real-time eye diagram capture and BER measurement. For the BER measurement of an IQ modulation format such as QPSK, the reported BER is the average of the separate measurements for I and Q components.

The narrow-band characteristic of the BA is illustrated in Fig. 4(a). The frequency the offset denotes the frequency drift away from the optimal Brillouin frequency shift in the SMF of the experiment, measured as 10.810 GHz. The BA gain drops to zero when the frequency offset is ∼45 MHz. Figure 4(b) shows the relationship between the Brillouin pump power and the BA gain, where a 150 mw pump produces a ∼40 dB gain on the pilot tone with −34 dBm power at the input of the 500 m SMF.

System performance is evaluated using 10 Gbaud BPSK and QPSK channels, each with −30 dB PSR. Figure 5(a) shows that the eye diagram opens and closes with $\Delta\theta$ between the two comb lines in Fig. 3(b4). Figure 5(b) presents the eye diagrams for different modulation formats. As a baseline for comparison, a 10 Gbaud BPSK signal with a residual carrier in the center is sent directly to the PD. Compared to the baseline system, the proposed SHD has a relatively higher noise level which is attributed to the extra spontaneous Brillouin noise during pilot tone boosting by BA. After a 100 km transmission, the signal quality degrades a little further, which might be caused by the residual chromatic dispersion of the link. By adjusting $\Delta\theta$, the I and Q components of the QPSK signal are obtained, as shown in Fig. 5(b).

The real-time BER of a 10 Gbaud channel is measured, as shown in Fig. 6(a). The received power is measured after the attenuator in the detector part of Fig. 3(a). Compared to the ideal case, the B2B BPSK has a similar BER curve. After the 100 km link, a power penalty of ∼0.5 dB is observed at the FEC limit (BER = 3.8 e^{-3}). For a QPSK signal, a power penalty of 4 dB is observed at the FEC limit. A BER comparison with a 20 Gbaud BPSK signal is shown in Fig. 6(b) to

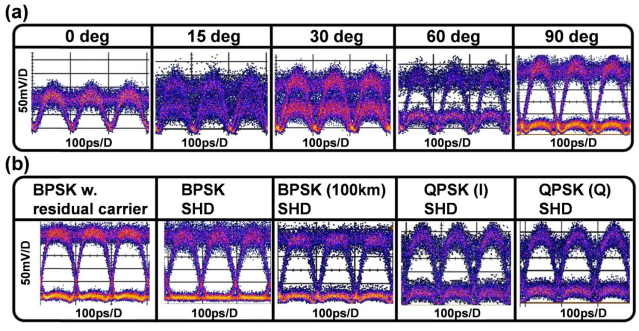

Fig. 5. (a) Detected eye diagram of BPSK varies with $\Delta\theta$ between two comb lines; (b) detected eye diagrams for a 10 Gbaud system with different modulation formats.

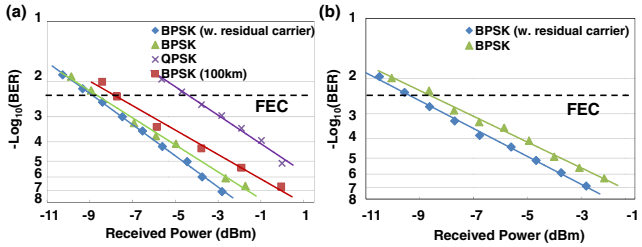

Fig. 6. BER for (a) 10 Gbaud BPSK/QPSK and (b) 20-Gbaud BPSK.

demonstrate the tunability of the scheme. Compared to the 20 Gbaud BPSK baseline, a power penalty of ~0.5 dB is observed at the FEC limit. Received power could also be measured before the BA stage (after the 100 km link). However, since the signal would experience degradation after two stages of SHD, the same received power would yield a higher BER. The result would be that, except for the baseline curve, the curves would have shifted to the right.

B2B system performance is also investigated for different PSRs, while the received power is kept at −8.4 dBm. Figure 7(a) shows that as PSR decreases, the power of the Brillouin pump needs to be increased to maintain the same output power of the amplified pilot tone. Therefore, the output PSR remains the same, which produces a relatively constant BER. The proposed scheme can even work with a PSR as low as −40 dB. When the PSR further decreases to −45 dB, the slave laser fails to lock to the faint input pilot tone, and the BER dramatically increases. The proposed scheme is also verified with Nyquist pulse shaping of 0.01 rolling off factor, as shown in Fig. 7(b). This scheme could potentially be extended to the WDM system with a low PSR, which requires multiple BA pumps to be generated accordingly [27]. It is noted that the pilot tone is separated from the data channel by a 40 GHz gap. For WDM applications, this placement may affect the spectrum efficiency. Moving the pilot tone closer to the data spectrum would alleviate this problem. However, the resultant interference from the data spectrum could degrade the quality of the pilot tone. Therefore, optimizing the location of the pilot tone requires further investigation.

In this Letter, BPSK/QPSK is employed only to demonstrate the concept of the proposed SHD system, which is based on high-speed optical nonlinear wave mixing. Compared to conventional differential detection [28] and digital phase tracking [29] for BPSK/QPSK, the SHD complexity might be higher. However, SHD is expected to relax encoder and decoder design restrictions in deferential detection schemes for MPSK signals [30]. In addition, SHD could be important

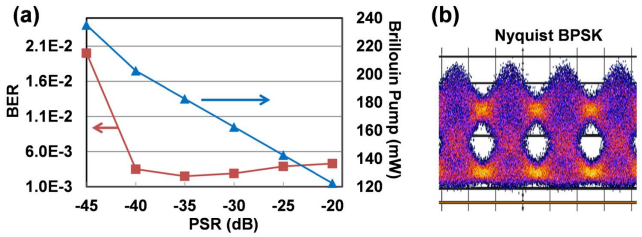

Fig. 7. (a) BER measurements for different levels of PSR and the corresponding Brillouin pump power with −8.4 dBm received power; (b) eye diagram of 10 Gbaud Nyquist BPSK signal.

for high-order QAM with an increased data rate, in which high-speed digital processing for phase tracking might be a challenge [12]. In addition, the ability of this approach to support multiple-channel SHD realization could be of interest in the future.

Funding. Center for Integrated Access Networks (CIAN); Fujitsu Laboratories of America (FLA); National Science Foundation (NSF).

REFERENCES

1. P. J. Winzer, IEEE Commun. Mag. **48**(7), 26 (2010).
2. E. Ip, A. Lau, D. Barros, and J. Kahn, Opt. Express **16**, 753 (2008).
3. M. G. Taylor, IEEE Photon. Technol. Lett. **16**, 674 (2004).
4. L. Kazovsky, J. Lightwave Technol. **4**, 182 (1986).
5. S. Ristic, A. Bhardwaj, M. J. Rodwell, L. A. Coldren, and L. A. Johansson, J. Lightwave Technol. **28**, 526 (2010).
6. M. Lu, H. Park, E. Bloch, A. Sivananthan, A. Bhardwaj, Z. Griffith, L. A. Johansson, M. J. Rodwell, and L. A. Coldren, Opt. Express **20**, 9736 (2012).
7. X. Zhou, IEEE Photon. Technol. Lett. **22**, 1051 (2010).
8. A. Viterbi, IEEE Trans. Inf. Theory **29**, 543 (1983).
9. I. Fatadin, D. Ives, and S. J. Savory, IEEE Photon. Technol. Lett. **22**, 631 (2010).
10. T. Pfau, S. Hoffmann, and R. Noé, J. Lightwave Technol. **27**, 989 (2009).
11. Z. Vujičić, R. S. Luís, J. Mendinueta, A. Shahpari, N. B. Pavlović, B. J. Puttnam, Y. Kamio, M. Nakamura, N. Wada, and A. Teixeira, IEEE Photon. Technol. Lett. **27**, 2226 (2015).
12. M. Nakamura, Y. Kamio, and T. Miyazaki, Opt. Express **16**, 10611 (2008).
13. A. Chiuchiarelli, M. Fice, E. Ciaramella, and A. Seeds, Opt. Express **19**, 1707 (2011).
14. K. Kasai, S. Beppu, Y. Wang, and M. Nakazawa, in *Optical Fiber Communication Conference*, OSA Technical Digest (Optical Society of America, 2015), paper W1E.4.
15. T. Kobayashi, A. Sano, A. Matsuura, Y. Miyamoto, and K. Ishihara, J. Lightwave Technol. **30**, 3805 (2012).
16. T. Huynh, L. Nguyen, V. Vujicic, and L. Barry, J. Opt. Commun. Netw. **6**, 152 (2014).
17. M. Chitgarha, A. Mohajerin-Ariaei, Y. Cao, M. Ziyadi, S. Khaleghi, A. Almaiman, J. Touch, C. Langrock, M. Fejer, and A. Willner, J. Lightwave Technol. **33**, 1344 (2015).
18. M. Ziyadi, A. Mohajerin Ariaei, M. Chitgarha, Y. Cao, A. Almaiman, Y. Akasaka, J. Yang, G. Xie, P. Liao, M. Sekiya, J. Touch, M. Tur, C. Langrock, M. Fejer, and A. Willner, in *Conference on Lasers and Electro-Optics (CLEO)*, San Jose, California, 2015, pp. 1–2.
19. Y. Cao, A. Almaiman, M. Ziyadi, P. Liao, A. Mohajerin Ariaei, F. Alishah, C. Bao, A. Fallahpour, B. Shamee, A. Willner, A. Youichi, T. Ikeuchi, S. Wilkinson, J. Touch, M. Tur, and A. Willner, in *Optical Fiber Communication Conference*, OSA Technical Digest (Optical Society of America, 2016), paper M2A.6.
20. N. A. Olsson and J. van der Ziel, Appl. Phys. Lett. **48**, 1329 (1986).
21. L. Banchi, M. Presi, R. Proietti, and E. Ciaramella, Opt. Express **18**, 12702 (2010).
22. G. Lu, T. Bo, T. Sakamoto, N. Yamamoto, and C. Chan, Opt. Express **24**, 22573 (2016).
23. X. Zhou and J. Yu, J. Lightwave Technol. **27**, 3641 (2009).
24. A. Albores-Mejia, T. Kaneko, E. Banno, K. Uesaka, H. Shoji, and H. Kuwatsuka, in *Proceedings of the European Conference on Optical Communication (ECOC)*, Cannes, 2014, paper Tu.3.1.4.
25. K. Kasai, Y. Wang, S. Beppu, M. Yoshida, and M. Nakazawa, Opt. Express **23**, 29174 (2015).
26. A. Leven, N. Kaneda, U. V. Kco, and Y. K. Chen, IEEE Photon. Technol. Lett. **19**, 366 (2007).
27. A. Lorences-Riesgo, M. Mazur, T. Eriksson, P. Andrekson, and M. Karlsson, Opt. Express **24**, 29714 (2016).
28. R. Griffin and A. Carter, in *Optical Fiber Communication Conference*, OSA Technical Digest (Optical Society of America, 2002), paper WX6.
29. R. Noé, J. Lightwave Technol. **23**, 802 (2005).
30. T. Miyazaki, IEEE Photon. Technol. Lett. **18**, 388 (2006).